Journal of Engineering Research and Reports

Volume 26, Issue 2, Page 89-106, 2024; Article no.JERR.111459
ISSN: 2582-2926

Interference Mitigation and Power Consumption Reduction for Cell Edge users in Future Generation Networks

Christopher O. Uloh [a*], Emmanuel A. Ubom [a], Akaniyene U. Obot [b] and Ubong S. Ukommi [a]

[a] Department of Electrical / Electronics Engineering, Akwa Ibom State University, Nigeria.
[b] Department of Electrical / Electronics Engineering, University of Uyo, Nigeria.

Authors' contributions

This work was carried out in collaboration among all authors. All authors read and approved the final manuscript.

Article Information

DOI: 10.9734/JERR/2024/v26i21074

Open Peer Review History:
This journal follows the Advanced Open Peer Review policy. Identity of the Reviewers, Editor(s) and additional Reviewers, peer review comments, different versions of the manuscript, comments of the editors, etc are available here: https://www.sdiarticle5.com/review-history/111459

Original Research Article

Received: 12/11/2023
Accepted: 15/01/2024
Published: 27/01/2024

ABSTRACT

In 5G heterogeneous networks (HetNets), a unique and promising option to address the growing demand for higher data rates is network densification of small cells (SCs) and macro cells (MCs). Unfortunately, the 5G HetNets are suffering severe issues due to the interference caused by these densely populated SCs and their high-power consumption. To lessen interference and boost network throughput, a New Soft Frequency Reuse (NSFR) technique is put forth in this work. The proposed scheme uses the Soft Frequency Reuse (SFR) for on/off switching of the SCs according to their Interference Contribution Rate (ICR) values. By splitting the cell region into edge and center zones, it resolves the interference issue caused by the densely packed SCs. Moreover, SC on/off switching addresses the issue of excessive power consumption and improves the 5G network's power efficiency. Furthermore, this work tackles the irregular shape nature problem of 5G HetNets and compares two different proposed shapes for the centre zone of the SC, existing irregular and proposed circular shapes. Additionally, the optimum radius of the centre zone, which maximizes the

**Corresponding author: Email: christopheruloh2016@gmail.com;*

total system data rate, is obtained. A comparative analysis of power consumption, data rate and power efficiency was performed between the NSFR model, the SFR model and the proposed model. The results show that for 1000 number of equipment, the proposed model has a low power consumption of 1.72KW compared to 3.51KW for SFR and 3.73KW for NSFR. Data rate of 12.19kbps compared to 11.42kbps for SFR and 11.09kbps for NSFR. Also, power efficiency of 610kbps/W compared to 572kbps/W for SFR and 560kbps/W for NSFR. These results imply that the interference mitigation handled by the proposed scheme improves by approximately 22%.

Keywords: 5G cellular network; small cells; macro cells; SFR model; NSFR model.

1. INTRODUCTION

An average of 0.01% of new user equipment is added to telecommunications networks daily [1]. The cumulative effect of this increase on devices which are connected to the 5G (5th Generation) network poses some pertinent issues in the network system which warrant system upgrades in terms of capacity, efficient energy consumption, and well-regulated data rates. Over the years, a series of research has been conducted on wireless telecommunications, diffraction loss, path length and other related issues [2,3]. Furthermore, research has shown that the number of devices connected to the 5G network will be between 10 and 100 times higher than what is obtainable in 4G networks and the data rates will increase up to 10 Gbps [1,4].

Research has shown that the study of past and current events is a prerequisite for predictions [5] and in that light, it has been predicted that by the year 2030, the communication sector will contribute to about 51% of global electricity consumption [6]. Consequently, researchers have invested quality efforts to investigate and develop some approaches to manage the upcoming overhead in the communication sector and by extension, the power sector. Such approaches include; Massive Multi-Input Multi-Output (MIMO) systems [7] and Millimetre Wave (mm-wave) [8] technologies. These researchers [9] made significant breakthroughs in their approach, which portrayed small cells as a novel technique with high efficiency in 5G services. However, their approach still leaves some footprints of challenges in the area of power consumption within the small cells and high interference between the cells. To address the power consumption problem, another group of researchers [10] surveyed open issues in energy efficiency of 5G networks and the group in [11] implemented sleep mode switching in small cells. Several degrees of sleep depth were also proposed in [12]. These sleep strategies were only effective where there were macro cells. Small cells wake up when macro cells are overloaded. Invariably, the sleep mode strategy does not function where there is no macro cell. A sleep mode-based resource allocation strategy was proposed by Liu [13]. In their method, an interference map was formed to select disabled femtocells, but the shortcoming of this method is the inability to update the map on disabled femtocells which results in a non-optimal solution.

In contrast to the preceding approaches, a separate study [14] explores a dynamic energy-saving method for 5G HetNets. This method optimises sleep mode based on traffic loads, relying on analysing the traffic distribution across smaller cells (SCs). This technique depends on cell-to-cell communication using X2 links that aim to switch off the cells with minimum load. Building upon existing research, [15] introduces a novel Q-learning-based technique for adjusting traffic loads in 5G HetNets. This technique dynamically shifts workload between busy and idle small cells, striving to maximize the number of cells in sleep mode while ensuring service quality. Seeking a balance between power consumption and network performance, [16] introduces an innovative energy-aware scheme. This scheme relies on pre-defined capacity thresholds to dictate when BSs are switched on, balancing energy savings with effectively meeting user demands. While [17] proposes a unique and simple sleep mode strategy for small cells, its effectiveness relies on their deployment beneath larger, main cells. The scheme falls short when main cells are absent, limiting its applicability.

A new sleeping strategy was demonstrated in [18] to precisely determine the SCs located in unwanted interference spots and deactivate them to enhance the capacity and energy efficiency in HetNets. Researchers in [19] developed a rule-based, energy-efficient algorithm for allocating resources in small cell networks. This algorithm enables both small cells and the main cell to

leverage the same spectrum, but with safeguards in place to maintain a baseline quality of service for users on the main cell. Soft frequency reuse (SFR) was introduced in [20,21] as a solution to the interference problem in HetNets. [20] explored a Soft Frequency Reuse (SFR)-based approach to tackle two key challenges in cellular networks: minimizing interference between cells and optimizing energy efficiency. Researchers in [21] came up with a clever way to reduce interference in cell networks. They divide cells into smaller circles and assign specific power and frequency ranges to each, creating a patchwork quilt of optimized resources.

The shortcomings of the aforementioned techniques which include a high level of complexity especially for antenna designs, and time investment in assembly lines arouse the interest in this research to investigate and propose a novel method to ameliorate the core system metrics while keeping its design and implementation simple and efficient.

This research aims to reduce interference mitigation and power consumption in 5G networks. To achieve this aim, the following objectives were followed: developed network cell segmentation scheme for interference mitigation and power reduction for cell edge users in 5G heterogeneous network using interference contribution rate technique for small cells switching control; developed and evaluated shape-based model using cluster vertices formation for small cell; developed centre zone determination mechanism for various shapes of network zones; computed the optimal radius of the zone centroid hence, improved the overall system data rate; and benchmarked the proposed method with other existing methods.

2. METHODOLOGY

2.1 Model Overview

The model simulation and validation were performed using Matrix Laboratory (MATLAB). The selected parameters adopted for the simulation are presented in Table 1. In the simulation environment, macro cells were created and they contained small cells according to the model design presented in Fig. 1. The target network area had users' equipment arbitrarily distributed.

This research used experimental methodology for interference mitigation and power consumption reduction for cell edge users in a 5G network using a Network cell Segmentation scheme (NetSc), with the heterogeneous network as the network type considered. In the simulation environment, macro cells were created and they contain small cells (SCs) as presented in Fig. 1. The target network area had user equipment arbitrarily distributed. The small cells were mounted within a network region marked as macro cells (MCs) which were designed to operate within the low-frequency band to achieve a wide coverage area. On the other hand, a high frequency band formed the operating region of the SCs and this is to ensure that a substantial network capacity is obtained.

The frequency band variation between SCs and MCs cancels out any interference that may exist between them. To avoid drift in the coverage area during SC switching, MCs must be kept alive always. As a backup solution, an effective handover scheme is required for all user equipment (UE) contained in the dead SC. If there are available channels in the MC, the user equipment in the dead SC should be moved immediately to the MC. SCs can either be in an ON state or an OFF state. During the OFF (sleep) state, user equipment continuously receives a discovery signal by the active SCs while they transmit their channel state to the connected SC. The assumption that governs this information exchange is that the user equipment is within the communication area of the SC. In this research, SC switching is not considered to be arbitrary, hence, it is assumed that the scheduler manages the allocation of sub-bands to the SCs as well as their switching control. However, if the scheduler fails, the MCs oversee the information collation from the SCs and control the sub-band sharing and SCs switching.

Considering the model in Fig. 1, it is impossible to compute the transmission power of any small cell without considering the signal-to-noise ratio as well as interference from neighbouring cells. In general engineering terms, signal-to-noise ratio (SNR) can be defined as the ratio of the useable power level to noise level and can be expressed mathematically as:

$$SNR = \frac{P_0}{N_0} \quad (1)$$

Where, P_0 denotes output power level, N_0 denotes interference or noise level measured in dB.

Table 1. Simulation parameters

Parameter	Value
Total number of small cells	200
Total number of user equipment	$100 - 1000$
Small cell idle index ($\boldsymbol{\phi}$)	0.52
Resource segment bandwidth	$200kHz$
Total number of resource segments	100
Overall bandwidth	$20MHz$
Base station power amplifier efficiency ($\boldsymbol{\eta}$)	0.52
Noise power spectral density	$-180dBm/Hz$
Power consumption gradient based on load ($\boldsymbol{\sigma}$)	6
Path loss between small cell and user equipment	$150.2 + 40.1\log_{10}(d)\ (db)$; d represents the distance (Km) between the considered small cell and user equipment
Transmission power of small cells	$20dBm$

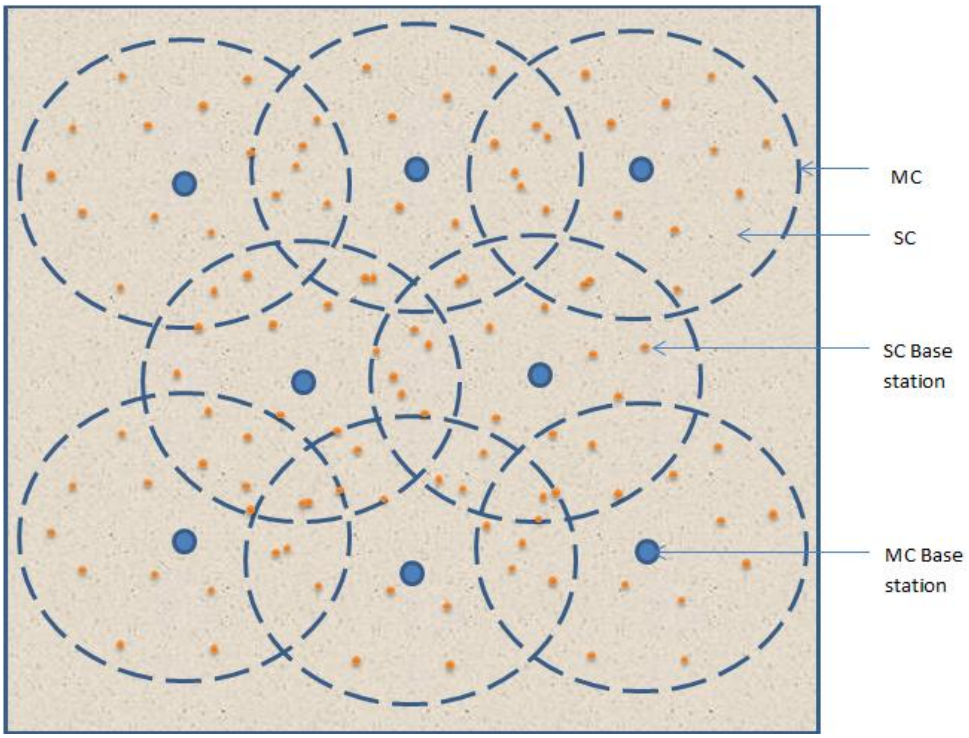

Fig. 1. Heterogeneous network system model

Consider a collection of SCs and a collection of user equipment which will be represented by $\chi_{SC}$and ψ_u, respectively. The concept in Equation 1 can be applied to obtain the signal-to-noise ratio for any user equipment within a small cell. Before the computation of signal-to-noise ratio the small cell switching concept is considered since the small cells can either go on or off. Let the small cell switching factor be denoted by δ_{sw} and its value at any given time is regulated by Equation 2 and signal to noise ratio for user equipment within a given small cell can be computed by Equation 3 [22].

$$\delta_{sw} = \begin{cases} 1 & if\ SC\ is\ on \\ 0 & if\ SC\ is\ off \end{cases} \quad (2)$$

$$SNR_{SC,UE} = \delta_{sw} \cdot G \cdot \left(\frac{P_{SC}}{\sum P + N_0 BW}\right) \quad (3)$$

Where, G denotes gain, P_{SC} is the transmission power of the small cell, P is the overall transmission power, N_0 denotes the noise element, and BW denotes the bandwidth assigned to the user equipment.

A specific quantity of resources must be allocated to user equipment according to the

user's required data rate. This is necessary to avoid a bridge in quality of service (QoS). In any given small cell, the data rate of user equipment in that cell can be calculated as given in Equation 4 [22].

$$DR = BW_{RS} \cdot \log_2\left(1 + SNR_{SC,UE}\right) \quad (4)$$

Where, RS denotes the resource segment and BW_{RS} denotes the bandwidth of the resource segment.

To get the least data rate needed by the user equipment, the knowledge of the resource segment for that equipment is required, and this can be computed as the ratio of the minimum data rate needed by the user equipment to the data rate of the user equipment within the considered small cell. This is represented mathematically as Equation 5 [22].

$$N_{RS} = ceil\left(\frac{DR_{UE_{min}}}{DR}\right) \quad (5)$$

Where, $DR_{UE_{min}}$represents the smallest data rate needed by the user equipment.

The downscaling operator (ceil) in Equation 5 is applied to ensure that the least integer is returned by the function. In any given small cell, the data rates can be computed as the summation of data rates of user equipment as in Equation 6 [22].

$$DR_{SC} = \sum DR_{UE} \quad (6)$$

By applying Shanon's computation methods Equation 6 can be modified to Equation 7.

$$DR_{UE} = BW \cdot \log_2 e^0 + BW \cdot SNR_{SC,UE} \quad (7)$$

The reduction in noise power will increase$SNR_{SC,UE}$, and consequently, an increase in data rate will be realized. The overall power in the small cell in active mode can be computed as in Equation 8 [22].

$$P_{SC_{on}} = P_{TH} + \alpha_L \cdot \alpha_{amp} \cdot P_{nom} \quad (8)$$

Where, P_{TH} is the threshold power, α_L is the power loss factor, α_{amp} is the power amplification factor, and P_{nom} is the nominal power consumption.

Although small cells can be in a sleep state, power consumption can still be obtained but negligible. In the sleep state, power consumption in small cells can be computed as in Equation 9 [22].

$$P_{SC_{off}} = P_{TH} \cdot \varepsilon \quad (9)$$

Where, ε represents the depth of idleness of the small cell.

Thus, the overall power consumption of a small cell is computed as Equation 10 [22].

$$P_{SC_T} = \sum_{t_1}^{t_{max}} P_{SC_{off}} + (1-\varepsilon) \sum_{t_1}^{t_{max}} P_{SC_{on}}\, t_1 < t_{max} \quad (10)$$

Where, t_1 is any initial time that could be considered and t_{max} is any final time that could be considered, and the constraint $t_1 < t_{max}$ must be strictly followed.

The first part of Equation 10 computes the total time when the small cells stay off. Similarly, the total power during the active period is computed in the second part of Equation 10. The lower and the upper time boundaries allow the power consumption to be computed for any range of time. The expanded form of Equation 10 can be expressed as Equation 11 [22].

$$P_{SC_T} = \sum_{t_1}^{t_{max}} P_{TH} \cdot \varepsilon + (1-\varepsilon) \sum_{t_1}^{t_{max}} \alpha_L \cdot \alpha_{amp} \cdot P_{nom}\, t_1 < t_{max} \quad (11)$$

Transmission power P_{nom} of a small cell which is a member of the second part in Equation 11 can be computed as Equation 12 [23].

$$P_{nom} = \sum N_{RS} \frac{\sigma P_{max}}{\eta N_{RS_{max}}} \quad (12)$$

Where, σ denotes the residual power consumption as a result of load, P_{max} denotes the highest transmission power by small cell, $N_{RS_{max}}$ denotes the maximum number of resource segments, and η denotes the base station's amplifier efficiency.

To minimize interference in the target 5G network, this research applies some novel techniques to regulate the attenuation level for frequency handover above the sensitivity level. The interference effect of any small cell i_{SC} can be expressed as the ratio of small cell induced interference power to the sum of reference signal power of all active user equipment. This can be computed as in Equation 13 [23].

$$i_{SC} = \frac{P_{SC} \cdot G_{SC}}{\sum P_{UE} \cdot G_{UE}} \quad (13)$$

Where, P_{SC} is the transmission power of the small cell, G_{SC} is the gain in the mall cell, P_{UE} is the transmission power of user equipment, G_{UE} is the gain in user equipment.

Let $\mathbb{C}$ denote the correction factor to regulate the quantity of handover small cell switching, Equation 13 can be rewritten as Equation 14 [22].

$$i_{SC} = \frac{P_{SC} \cdot G_{SC}}{(\sum P_{UE} \cdot G_{UE}) \cdot \mathbb{C} \cdot N_{UE}} \quad (14)$$

Where, N_{UE} is the quantity of user equipment in a small cell.

From Equation 14, when $\mathbb{C} \cdot N_{UE}$ increases, it implies that the quantity of user equipment has increased. This will consequently reduce i_{SC} as well as the certainty level of the small cell off state.

2.2 Network Cell Segmentation (NetSc) Scheme

This research proposes the NetSc-based strategy to attenuate interference in a given 5G heterogeneous network. The effect of this mitigation will improve the overall efficiency of the system. In this scheme, the cells are organized to obtain centre and terminal clusters. Each cell is assigned an auxiliary band based on the NetSc algorithm. This design model is concerned with the reduction of interference around the small cells, thus, for each idle cluster; an active cell can use the sub-band around the terminals of the idle neighbouring cluster while reserving the remaining sub-band for the centre cluster. On the other hand, suppose the sub-band capacity is saturated by the terminal clusters, then each cluster of any small cell falls back to its sub-band. Every small cell and the corresponding macro cell can establish a network to share user equipment information and other measurements. The user equipment data and transmission rate are also made available to the router which decides on the small-cell switching. Small cell sub-band assignment can be performed using Algorithm 1.

Algorithm 1: Small cell sub-band Assignment

1: Begin
2: Initialize a collection of all possible sub-bands as $S_B \leftarrow 0$
3: Initialize a collection of all small cells as $U_{SC} \leftarrow 0$
4: Initialize a sub-band assigned to small cell as B_{SC}
5: for I = 0; i<$U_{SC}.length$; i++
6:locate a collection of used sub-band in the terminal cluster of the surrounding small cells and store it in a variable E_c
7:Compute a collection of the remnant sub-band for the terminal cluster of the active small cell as $R_c = S_B - E_c$
8:if $R_c.length > 1$then
9:for each sub-band r in R_c
10:Compute the nearest distance as d_{min} between the sub-band allocated to the target small cell and the closest small cell using the sub-band r within its terminal cluster.
11:Compute the sub-band with the maximum distance as r_{max}
12:$B_{SC} \leftarrow r_{max}$
13:end for
14:else if $R_c.length = 1$
15:$S_B \leftarrow R_c$
16:else
17:for each sub-band e in E_c
18:Compute the distance as d_e between the sub-band allocated to the target small cell and the surrounding small cell using the sub-band e within its terminal cluster.
19:Compute e_{max} such that e has the maximum distance d_e
20:$B_{SC} \leftarrow e_{max}$
21:end for
22:end if
23: end for

Algorithm 1 can be segmented into two main categories which are: the determination of the used sub-band in the terminal cluster of the surrounding small cells (line 6 and line 7) and the determination of the sub-band assigned to small cell (line 8 to line 20).

When any small cell is powered up, it detects its immediate surrounding small cell signal to obtain its sub-bands. This action is necessary by the newly powered small cell to avoid coincidental use of already used sub-band. Algorithm 1 identifies all used sub-bands and stores them in an array denoted as E_c while the free sub-bands are stored in R_c. The algorithm iterates through R_c to obtain the closest sub-band and the smallest cell using it. If all available sub-bands are assigned to the terminal cluster in the surrounding small cells, then the sub-band used by the farthest surrounding small cell is selected to reduce interference. The Middle cluster has the privilege to use the remaining sub-bands. This assignment procedure is further depicted in Fig. 2.

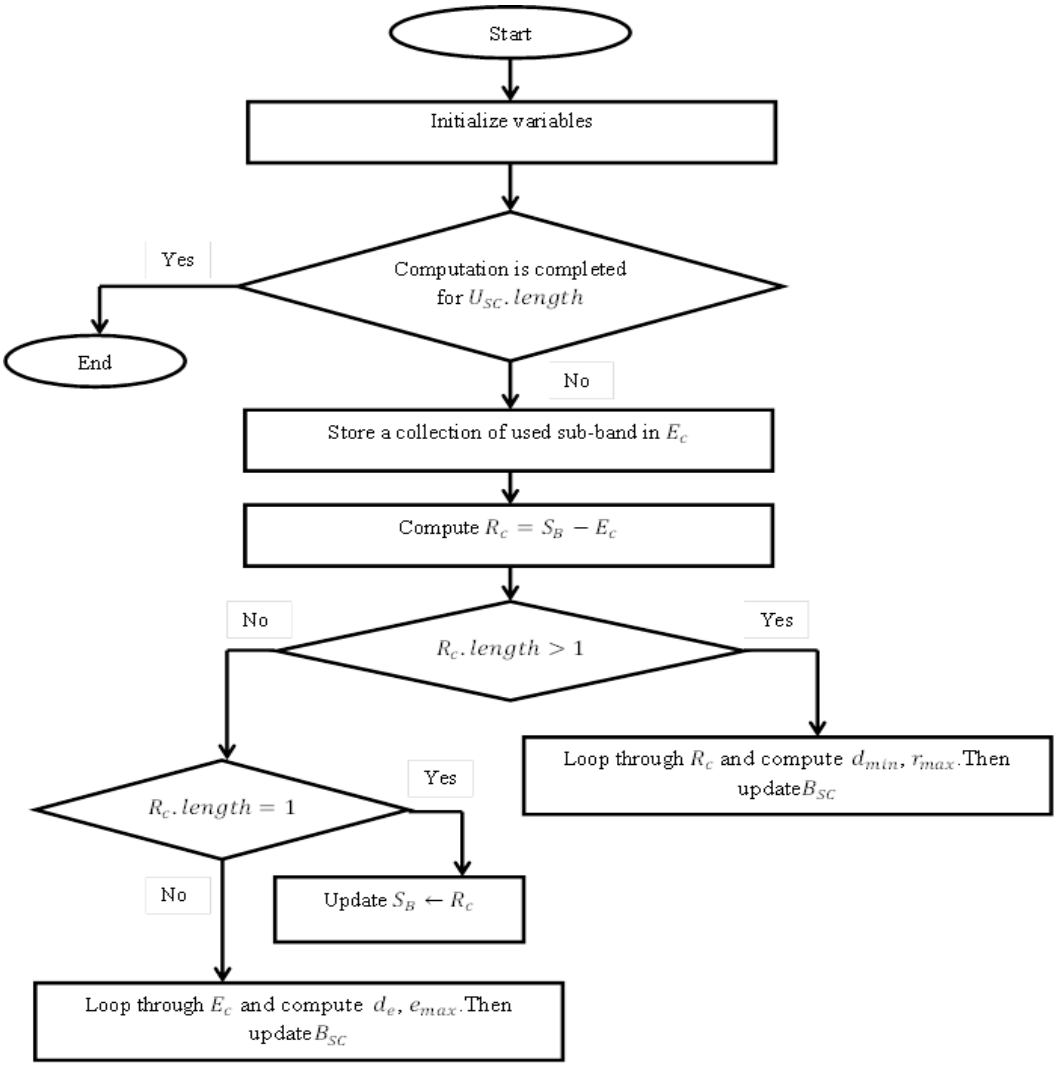

Fig. 2. Flowchart showing small cell sub-band assignment

2.3 Cluster Vertices Formation

The vertices of each cluster can be formulated to obtain either a circular-contoured cluster or an irregular-contoured cluster. The procedure for computation of middle cluster layout or contours and vertices is presented in Algorithm 2. The vertices of each cluster are constructed based on the cluster's radius. If the middle cluster has a similar contour to the terminal cluster, then the radius of the middle cluster can be computed as a partial length between every vertex and the middle of the small cell. To formulate the layout of the middle cluster, one major criterion is to compute the contour parameters. This procedure of obtaining a small cell vertex is performed for all the small cells whose vertices are to be determined. If the length between the vertex of the closest small cell and the middle of another small cell is obtained, then the closest acceptable distance is obtained.

Algorithm 2: Middle Cluster Determination Procedure

1: Begin
2: Define the collection of small cells as Z_{sc}
3: Define the middle small cell coordinate as $(x_{sc_{mid}}, y_{sc_{mid}})$
4: Define the coordinates of vertices as (x_{vert}, y_{vert})
5: Define small cell radius as r_{sc}
6: Define small cell vertex v_{sc}
7: Initialize [ ] $\leftarrow Z_{sc}$
8: Initialize $(0,0) \leftarrow (x_{sc_{mid}}, y_{sc_{mid}})$
9: Initialize $(0,0) \leftarrow (x_{vert}, y_{vert})$
10: Initialize $0 \leftarrow r_{sc}$
11: For each SC in Z_{sc}

12:if irregular-contoured cluster then
13:For each v_{sc} in SC
14:Compute the length of each vertex l_v with respect to the middle of the small cell
15:Compute the radius of the middle clustered small cell$r_{mid} = r_{sc} \times l_v$
16:Connect v_{sc} to middle SC
17:Compute $(x_{sc_{mid}}, y_{sc_{mid}})$: taken as the line intersection in Step 16
18:end for
19:else if circular-contoured cluster then
20:For each v_{sc} in SC
21:Compute the length of each vertex l_v with respect to the middle of the small cell
22:end for
23:compute the least l_v
24:compute $r_{mid} = r_{sc} \times least\ l_v$
25:Connect v_{sc} to middle SC
26:Compute $(x_{sc_{mid}}, y_{sc_{mid}})$
27:end if
28:end for
29:end

The middle cluster determination procedure presented in Algorithm 2 is further depicted in Fig. 3.

2.4 Power Consumption/Interference Management

To mitigate interference for cell edge users in a 5G network using Network Cell Segmentation, power management is essential. In the quest to keep the power consumption of the system at the barest minimum, this research adopts the small cell switching strategy. In this strategy, any small cell is switched on or off based on traffic and the rate of interference it produces. The small cell switching strategy is developed in Algorithm 3.

Algorithm 3: Small Cell Switching Procedure

1: Begin
2: Define the number of user equipment within the small cell as $N_{ue_{sc}}$
3: Define total load within the small cell as $L_{T_{sc}}$
4: Define load threshold within the small cell as $L_{THLD_{sc}}$
5: Defined maximum received signal strength in the small cell as $RSS_{max_{sc}}$
6: Define threshold received signal strength in small cell as $RSS_{THLD_{sc}}$
7: Define the rate of interference produced by small cell as ψ_{sc}
8: Define the average rate of interference produced by small cell as $\bar{\psi}_{sc}$
9: Define a set of all small cells as Z_{sc}
10: Define a set of all switched-off cells as $Z_{sc_{off}}$
11: Define a set of all switched-on cells as $Z_{sc_{on}}$
12: Define a set of all undefined state small cell as Z_{sc_u}
13: Initialize $0 \leftarrow N_{ue_{sc}}, L_{T_{sc}}, L_{THLD_{sc}}, RSS_{max_{sc}}, RSS_{THLD_{sc}}, \psi_{sc}, \bar{\psi}_{sc}$
14: Initialize [ ] $\leftarrow Z_{sc}, Z_{sc_{off}}, Z_{sc_{on}}, Z_{sc_u}$
15: For each$SC\ in\ Z_{sc}$
16: if$N_{ue_{sc}} = 0$then
17:$Z_{sc_{off}} \leftarrow SC$
18: else if $L_{T_{sc}} > L_{THLD_{sc}}\ ||\ RSS_{max_{sc}} > RSS_{THLD_{sc}}$then
19:$Z_{sc_{on}} \leftarrow SC$
20: else
21:$Z_{sc_u} \leftarrow SC$
22: end if
23: end for
24: For each $SC\ in\ Z_{sc_{on}}$
25: $\psi_{total_{sc}} \leftarrow \psi_{sc}$
26: end for
27: $\bar{\psi}_{sc} \leftarrow \psi_{total_{sc}} / Z_{sc_{on}}.Count$
28: For each $SC\ in\ Z_{sc_u}$
29: if $\psi_{sc} > \bar{\psi}_{sc}$then
30:Execute line 17
31:else
32:Execute line 19
33:Execute line 25
34:Execute line 27
35:end if
36:end for
37:end

In the small cell switching procedure presented in Algorithm 3, two major processes were highlighted. First, the state of all small cells was identified and each small cell was categorized based on state. There are three states in which a small cell can be (one at a time). These states are “on”, “off”, and “undetermined”. The pictorial illustration of Algorithm 3 is presented in Fig. 4.

The algorithm pushes any small cell into the “off” state if the number of user equipment within it is zero, as shown from line 16 to line 17, otherwise, the small cell is pushed into the “on” state as shown from line 18 to line 19. If the state of the small cell cannot be determined at any given time, then the small cell is pushed to the collection of undetermined state small cell object seen from line 20 to line 21. Line 24 to line 26 computes the total interference level of all small cells in the “on” state. The average interference level is computed in line 27.

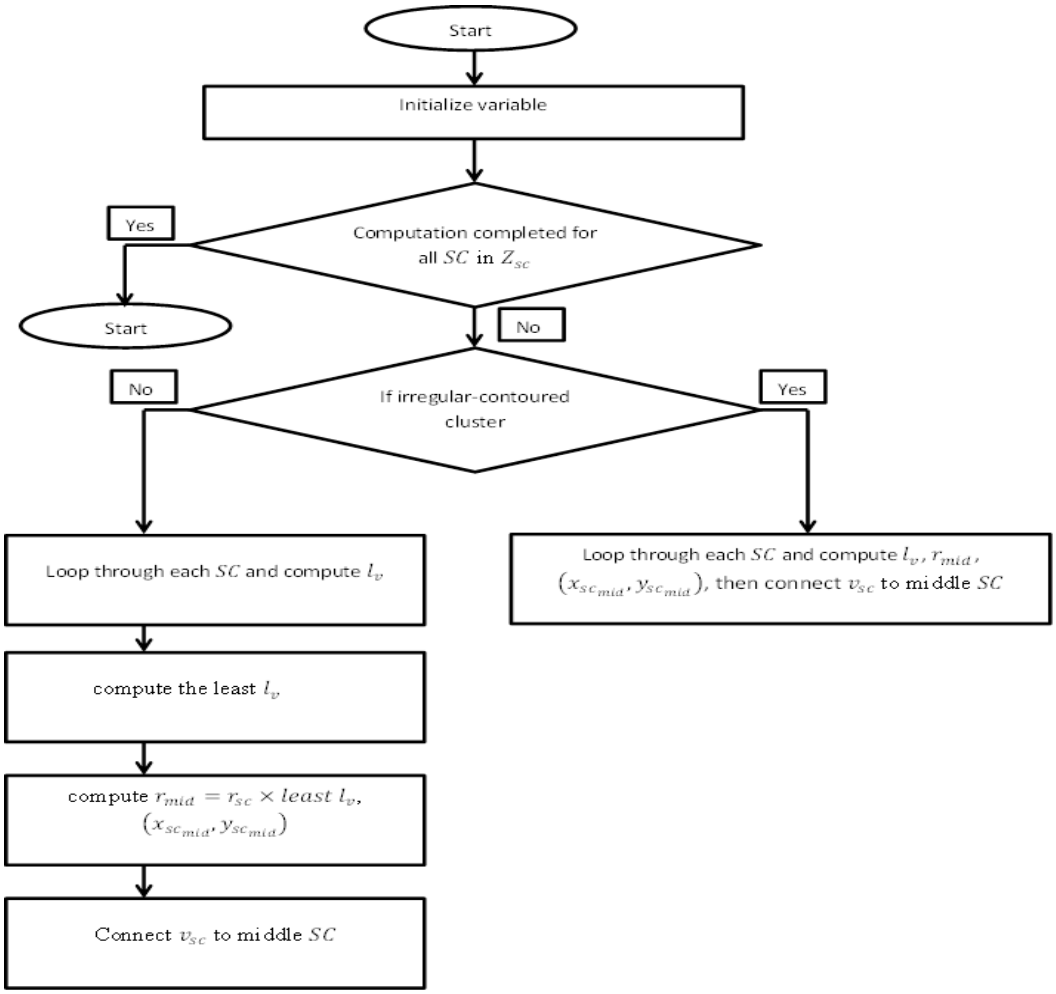

Fig. 3. Flowchart for middle cluster determination

Secondly, the algorithm further categorizes the small cells contained in the undetermined state object into “on” state and “off” state. The criteria the algorithm adopts for this categorization is based on the level of interference produced by the small cell. If the interference level in the small cell is greater than the average permissible interference level of all small cells in the “on” state, then the cell is switched off, otherwise, it is switched on. This cell state categorization is found from Line 28 to Line 33.

3. RESULTS AND DISCUSSION

3.1 Performance Analysis of the Proposed Irregular-Contoured and the Proposed Circular-Contoured Middle Cluster

The overall data rate with respect to the number of user equipment is presented in Table 2 and Fig. 5.

From the results obtained in Table 2, an average data rate of $5.995\ kbps$ was obtained for the circular-contoured cluster while $5.791\ kbps$ was obtained for the irregular-contoured cluster. The circular cluster has improved the data rate better than the irregular cluster.

Accordingly, the power consumption with respect to a number of user equipment is computed and the results are presented in Table 3 and Fig. 6.

The power consumption efficiency was estimated for various quantities of user equipment. Also, the failure probability for various signal-to-noise ratios is computed as a portion of user equipment which cannot meet the threshold signal-to-noise ratio. The failure probability computation was done based on Equation 15.

$$\rho_{failure} = \frac{\sum_c \sum_j \lambda_{j,c} \cdot SNR_{j,c}}{\sum_c \sum_j \cdot SNR_{j,c}} \quad (15)$$

Subject to

$$\begin{cases} \lambda_{j,c} = 1; & if\ SNR_{j,c} < SNR_{threshold} \\ \lambda_{j,c} = 0; & otherwise \end{cases}$$

Table 4 and Fig. 7 show that the circular-contoured cluster and the irregular-contoured cluster have close performance. This implies that the circular-contoured cluster model can be executed with confidence with an Omni-directional antenna.

Also, the failure probability for circular-contoured and irregular-contoured clusters is presented in Table 5 and Fig. 8.

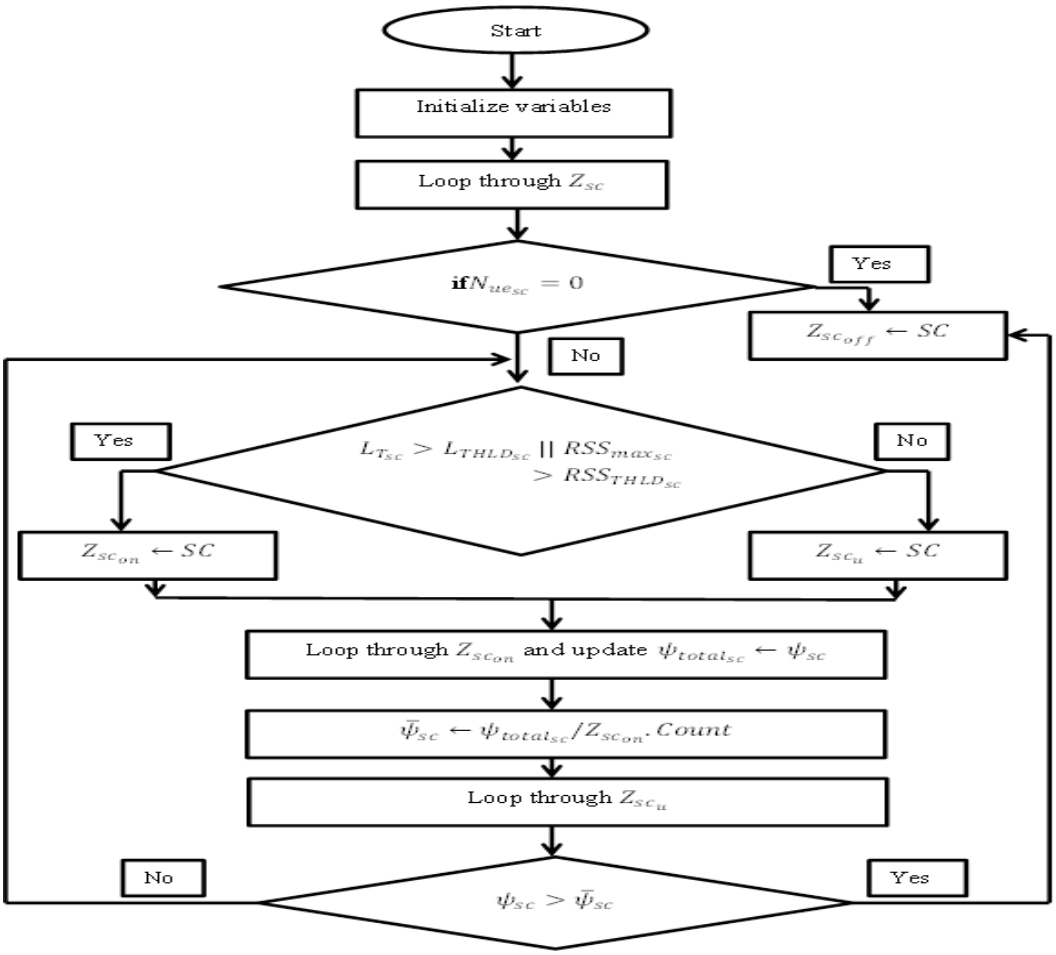

Fig. 4. Flowchart for small cell switching procedure

Table 2. Data rate versus number of user equipment for circular-contoured cluster and irregular-contoured cluster

Number of user equipment	Data rate (kbps)	
	circular-contoured cluster	irregular-contoured cluster
100	1.32	1.02
200	2.36	2.15
300	3.40	3.18
400	4.42	4.22
500	5.48	5.27
600	6.51	6.32
700	7.55	7.36
800	8.59	8.41
900	9.63	9.46
1000	10.69	10.52

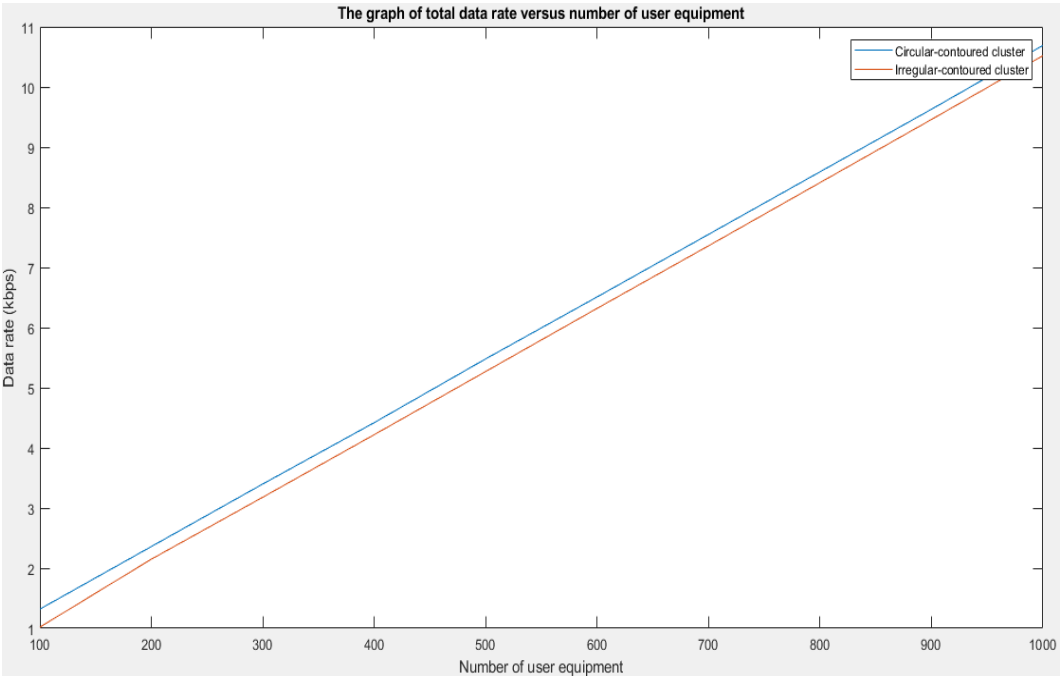

Fig. 5. Data rate versus number of user equipment for circular-contoured cluster and irregular-contoured cluster

Table 3. Power consumption versus the number of user equipment for circular-contoured cluster and irregular-contoured cluster

Number of user equipment	Power consumption (KW)	
	circular-contoured cluster	irregular-contoured cluster
100	1.30	1.28
200	1.35	1.32
300	2.00	1.97
400	2.50	2.48
500	3.00	2.87
600	3.52	3.48
700	4.10	4.07
800	4.51	4.49
900	5.20	4.98
1000	5.50	5.49

Table 4. Power efficiency for circular-contoured cluster and irregular-contoured cluster

Number of user equipment	Power efficiency (kbps/W)	
	circular-contoured cluster	irregular-contoured cluster
100	100	98
200	150	148
300	210	205
400	250	247
500	305	299
600	351	348
700	412	405
800	450	447
900	522	516
1000	551	549

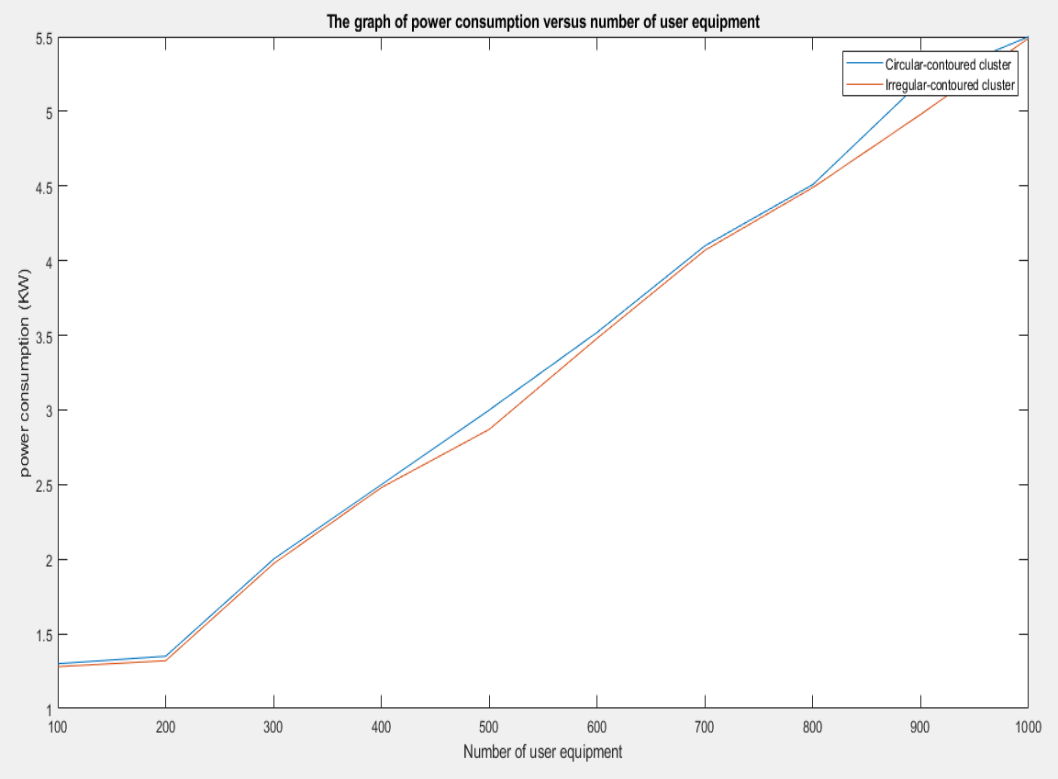

Fig. 6. Power consumption versus the number of user equipment for circular-contoured cluster and irregular-contoured cluster

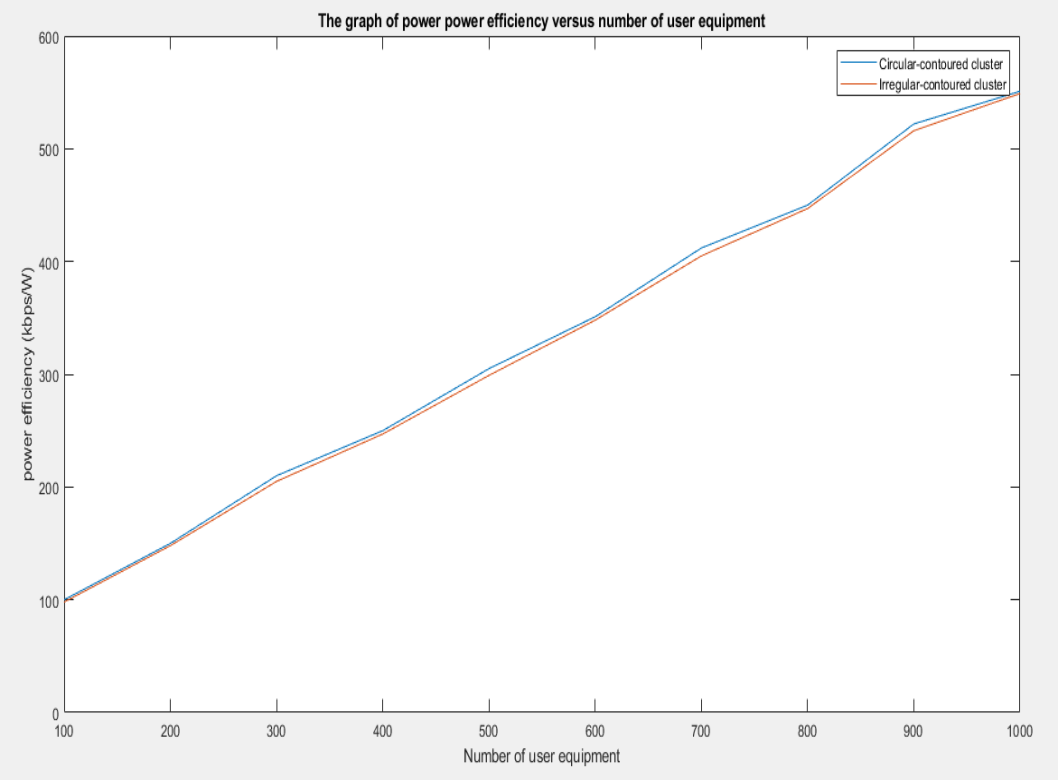

Fig. 7. Power efficiency for circular-contoured cluster and irregular-contoured cluster

Table 5. Failure probability for circular-contoured cluster and irregular-contoured cluster

Signal-to-noise ratio (dB)	Failure Probability	
	circular-contoured cluster	irregular-contoured cluster
1	0.10	0.12
5	0.15	0.17
10	0.30	0.32
15	0.51	0.52
20	0.72	0.73
25	0.84	0.84
30	0.91	0.93
35	0.96	0.95

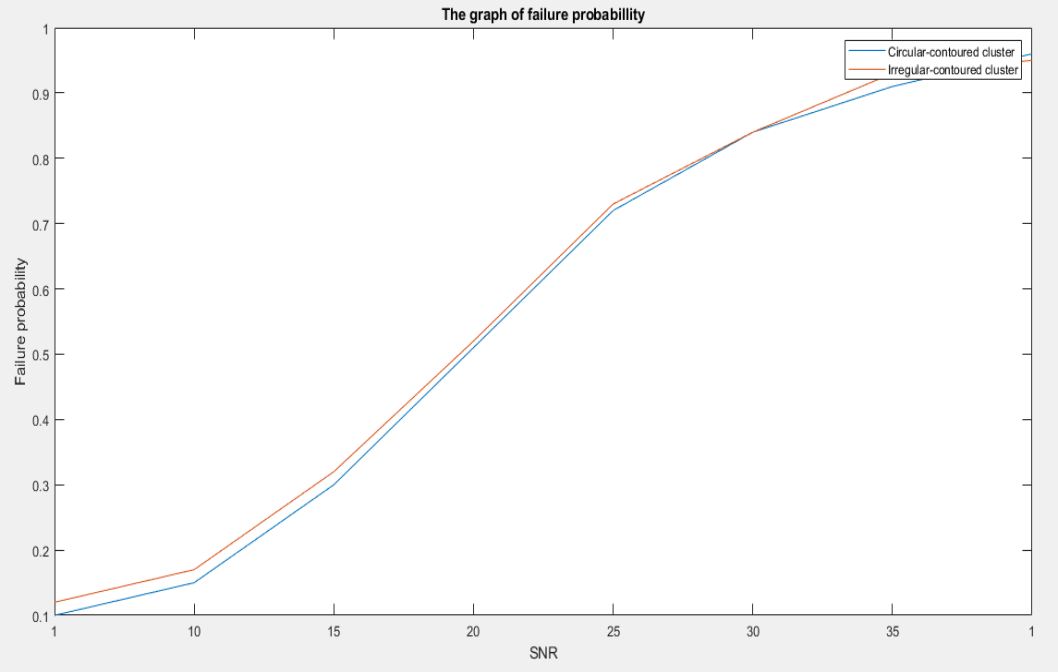

Fig. 8. Failure probability for circular-contoured cluster and irregular-contoured cluster

Average power efficiency and average failure probability were computed, and $330.1\ kbps/W$ and 0.5613 were obtained respectively, for circular-contoured cluster while $326.2\ kbps/W$ and 0.5725 were obtained respectively for the irregular-contoured cluster. The performance closeness of the two methods gives a high reliability on the circular-contoured cluster method.

3.2 Performance Analysis of Small Cell Switching Scheme

The power consumption of small cells was evaluated based on different user equipment and the results were compared with other schemes as shown in Table 6 and Fig. 9. The results show that power consumption is a function of user equipment. This relationship exists since transmission power becomes high if user equipment increases. The No Soft Frequency Reuse (NSFR) scheme developed by [1] consumes more power as shown in the results (Fig. 9). This is because all the small cells simultaneously are active always. The soft frequency reuse (SFR) scheme developed by [4] consumes less power compared to the NSFR scheme. This is because the SFR scheme is designed to allow low transmission power at the middle cluster. However, all small cells remain active always, thereby consuming more power. From Fig. 9, the proposed scheme (Small Cell Switching Scheme) has the lowest power consumption. This is because small cells are turned off when they are idle or have a higher interference. Small cells are turned off due to the high interference rate allocated to the user equipment within it to the nearest active small cell.

Table 6. Power consumption versus the number of user equipment

Number of User Equipment	Power Consumption (KW)		
	NSFR scheme	SFR scheme	Proposed scheme
100	1.72	1.51	1.01
200	1.90	1.69	1.09
300	2.15	1.87	1.15
400	2.27	2.14	1.23
500	2.51	2.29	1.31
600	2.77	2.50	1.39
700	3.01	2.72	1.47
800	3.24	3.02	1.55
900	3.50	3.22	1.63
1000	3.73	3.51	1.72

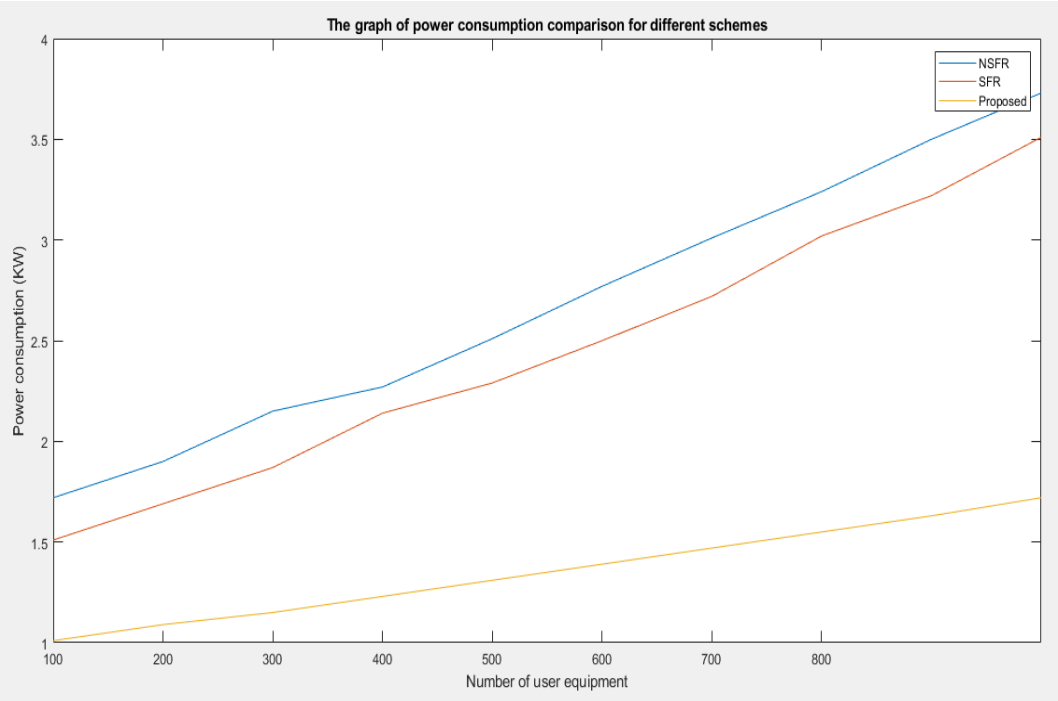

Fig. 9. Power consumption versus the number of user equipment

Table 7. Data rate comparison for various schemes

Number of User Equipment	Data Rate (kbps)		
	NSFR scheme	SFR scheme	Proposed scheme
100	1.72	1.92	2.82
200	2.76	3.05	3.95
300	3.80	4.08	4.88
400	4.82	5.12	6.02
500	5.88	6.17	7.08
600	6.91	7.22	8.13
700	7.95	8.26	9.17
800	8.99	9.31	10.22
900	10.03	10.36	11.28
1000	11.09	11.42	12.19

Table 7 and Fig. 10 shows the system data rates with respect to user equipment. The results show that the proposed scheme has the highest data rate as the interference level is lowest here. On the other hand, the NSFR scheme has the lowest data rate and the highest interference level.

The results in Fig. 8 show the power consumption of various schemes. It is necessary to evaluate the power efficiency of these schemes. Hence, the result showing the power efficiency of each of the considered schemes is presented in Table 8 and Fig. 11.

A comparative analysis of power consumption, data rate and power efficiency was performed between the NSFR model, the SFR model and the proposed model. The results show that the proposed model has low power consumption compared to the other two methods, and consequently, a high data rate which implies that the interference level is low, and with a high power efficiency. The results presented in Fig. 10 show that the interference mitigation handled by the proposed scheme improves by about 22%.

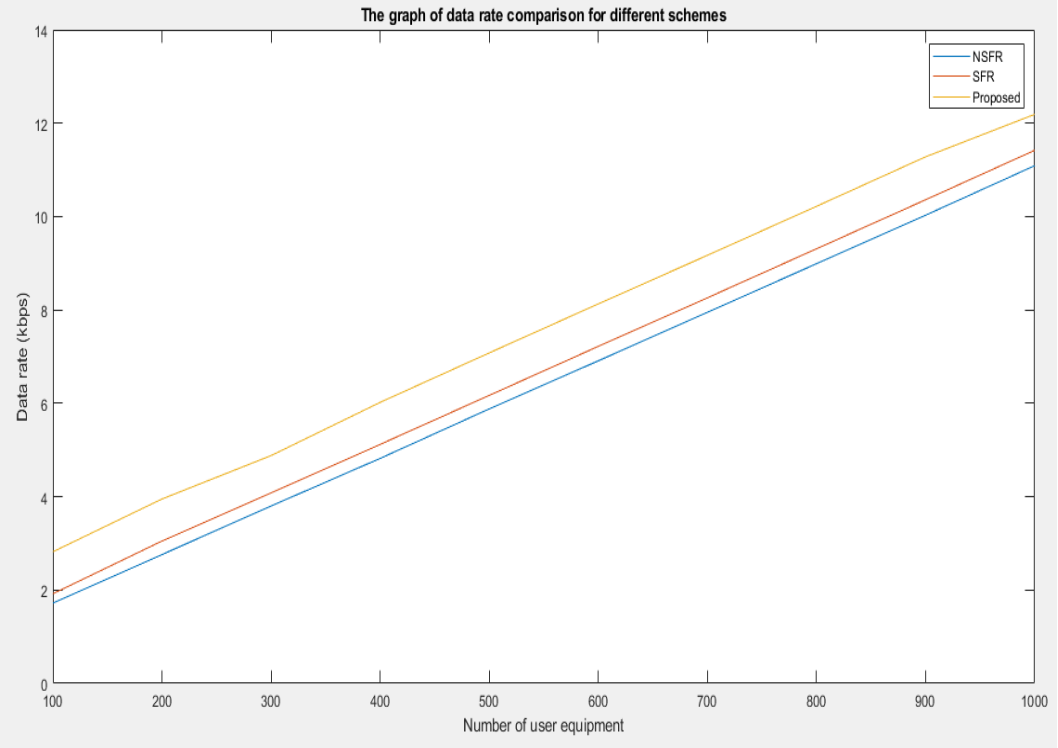

Fig. 10. Data rate comparison for various schemes

Table 8. Power efficiency comparison of various schemes

Number of User Equipment	Power Efficiency (kbps/W)		
	NSFR scheme	SFR scheme	Proposed scheme
100	108	112	152
200	158	160	202
300	215	227	264
400	257	270	302
500	310	322	363
600	359	370	405
700	418	429	472
800	459	470	505
900	527	538	580
1000	560	572	610

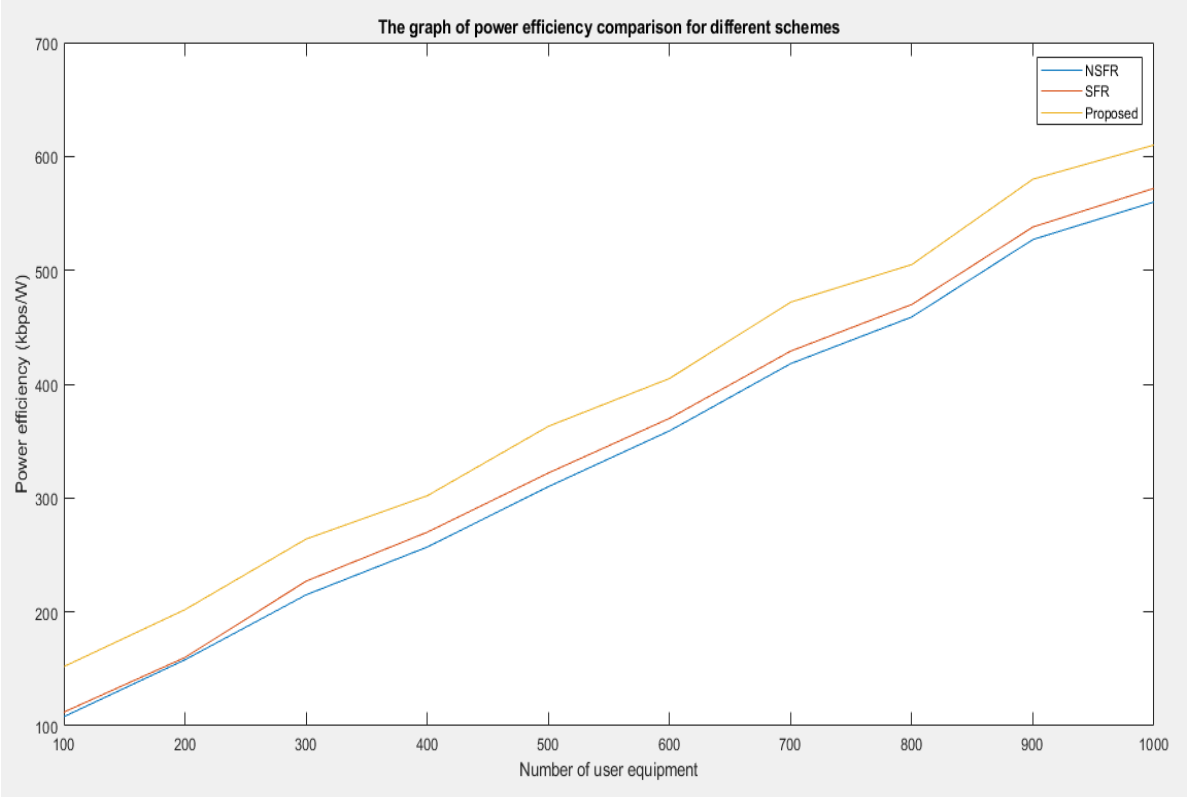

Fig. 11. Power efficiency comparison of various schemes

4. CONCLUSION

The implications of cluster formation have been extensively analyzed in this research. Specifically, two categories of these formations were considered namely: circular-contoured cluster and irregular-contoured cluster. Although the irregular-contoured cluster does not have a realistic implementation, its application to this research is based on a theoretical perspective and is to be used as a benchmark tool for a more realistic solution. On the other hand, the circular-contoured clustering technique – a more realistic approach in terms of implementation is presented in this research. Various metrics were used to measure the comparative performances of these two methods.

From the results, an average data rate of $5.995\ kbps$ was obtained for the circular-contoured cluster while $5.791\ kbps$ was obtained for the irregular-contoured cluster. Average power consumption of $3.298\ KW$ was obtained for the circular-contoured cluster and $3.243\ KW$ was obtained for the irregular-contoured cluster model. Similarly, average power efficiency and average failure probability were computed, and $330.1\ kbps/W$ and 0.5613 were obtained respectively, for circular-contoured cluster while $326.2\ kbps/W$ and 0.5725 were obtained respectively for the irregular-contoured cluster. The performance closeness of the two methods gives a high reliability on the circular-contoured cluster method.

The NSFR model, SFR model, and the suggested model were compared in terms of power efficiency, data rate, and consumption. With 1000 equipment, our proposed model shines with significantly lower power consumption (1.72KW) compared to SFR (3.51KW) and NSFR (3.73KW). It also boasts higher data rates (12.19kbps) than SFR (11.42kbps) and NSFR (11.09kbps), and a superior power efficiency of 610kbps/W compared to SFR (572kbps/W) and NSFR (560kbps/W). These impressive results suggest a roughly 22% improvement in our scheme's ability to handle interference. For future considerations, we can further optimize zone definition by considering User Equipment

distribution and signal strength, as well as tackling coverage gaps within Voronoi cells.

COMPETING INTERESTS

Authors have declared that no competing interests exist.

REFERENCES

1. Fourati H, Maaloul R, Chaari L. A survey of 5G network systems, challenges and machine learning approaches, International Journal of Machine Learning and Cybernetics. 2021;385-431.
2. Oloyede S, Ozuomba C, Kalu. Shibuya method for computing ten knife edge diffraction loss, software engineering. 2017;5(2):38-43.
3. Simeon O. Analysis of effective transmission range based on hata model for wireless sensor networks in the C-Band and Ku-Band. Journal of Multidisciplinary Engineering Science and Technology. 2020;7(12): 13673-13679.
4. Dee Ree M, Mantas G. A. Radwan, S. Mumtaz, J. Rodriguez and I. Otung, Key Management for Beyond 5G Mobile Small Cells: A Survey, IEEE Access. 2019; (7):59200-59236.
5. Oloyede S, Ozuomba P, Asuquo L. Olatomiwa and O. Longe, Data-driven techniques for temperature data prediction: big data analytics approach, Environ Monit Assess. 2023;195-343:1-21,
6. Andrae and T. Edler, On global electricity usage of communication technology: Trends to 2030. Challenges. 2015; 6(1):117-157.
7. Sheikhzadeh S, Javan M. Key Technologies in 5G: Air Interface. Modares Journal of Electrical Engineering. 2016;16(2):50-61.
8. Wong V, Schober R, Ng W, Wang L. Key technologies for 5G wireless systems, Cambridge, U.K.: Cambridge University Press; 2017.
9. Al-Falahy N, Alani O. Technologies for 5G Networks: Challenges and Opportunities. IT Professional. 2017;19(1):12-20.
10. Stoynov V, Poulkov V, Iliev G, Koleva P. Ultra-Dense Networks: Taxonomy and Key Performance Indicators. Symmetry. 2022; 15:1.
11. Yu W, Xu H, Zhang H, Griffith D, Golmie N. Ultra-Dense Networks: Survey of State of the Art and Future Directions, in 25th International Conference on Computer Communication and Networks (ICCCN), California; 2016.
12. Usama M. A survey on recent trends and open issues in energy efficiency of 5G," Sensors. 2018;19(14):3126.
13. Liu B Natarajan, Xia H. Small cell base station sleep strategies for energy efficiency. IEEE Transactions on Vehicular Technology. 2016;65(3):1652-1661.
14. Celebi H, Güvenç I. Load analysis and sleep mode optimization for energy-efficient 5G small cell networks, in IEEE International Conference on Communications Workshops (ICC Workshops), Paris; 2017.
15. Zhang Q, Xu X, Zhang J, Tao X, Liu C. Dynamic Load Adjustments for Small Cells in Heterogeneous Ultra-dense Networks, in IEEE Wireless Communications and Networking Conference (WCNC), Seoul; 2020.
16. Rehan S, Grace D. Efficient Joint Operation of Advanced Radio Resource and Topology Management in Energy-Aware 5G Networks, in IEEE 82nd Vehicular Technology Conference (VTC2015-Fall), Boston; 2015.
17. Lin Y, Wang L, Lin P. SES: A novel yet simple energy saving scheme for small cells. IEEE Transactions on Vehicular Technology. 2017;66(9):8347-8356.
18. Ebrahim, Alsusa E. Interference and resource management through sleep mode selection in heterogeneous networks. IEEE Transactions on Communications. 2017;65 (1):257-269.
19. Saeed E, Katranaras A, Zoha A, Imran M Imran, Dianati M. Energy efficient resource allocation for 5G Heterogeneous Networks, in IEEE 20th International Workshop on Computer Aided Modelling and Design of Communication Links and Networks (CAMAD), Guildford; 2015.
20. Huo L, Jiang D, Lv Z. Soft frequency reuse-based optimization algorithm for energy efficiency of multi-cell networks, Computers & Electrical Engineering. 2018; 66:316-331.
21. Malini and K. Babu, Soft frequency reuse based interference minimization technique for long term evolution-advanced heterogeneous networks,

in International Conference on Communication and Signal Processing (ICCSP), Chennai; 2017.

22. Shen Z, Lei X Huang, Chen Q. An Interference Contribution Rate Based Small Cells On/Off Switching Algorithm for 5G Dense Heterogeneous Networks. IEEE Access. 2018;6(1):29757-29769.

23. Huo L, Jiang D, Lv Z. Soft frequency reuse-based optimization algorithm for energy efficiency of multi-cell networks, Computers & Electrical Engineering. 2018;66:316-331.

Peer-review history:
The peer review history for this paper can be accessed here:
https://www.sdiarticle5.com/review-history/111459